

Insights into the adsorption-assisted PMS activation of Ce-UiO-66-4F in in-situ chemical oxidation process for efficient pollutants removal

Dong Wang^{a,b}, Soliu O. Ganiyu^b, Xuefen Wang^{a,*}, Mohamed Gamal El-Din^{b,*}

*a State Key Lab for Modification of Chemical Fibers and Polymer Materials,
College of Materials Science and Engineering, Donghua University, Shanghai,
201620, P.R. China*

*b Department of Civil and Environmental Engineering, University of Alberta,
Edmonton, AB T6G 1H9, Canada*

*Corresponding author.

E-mail address: wangxf@dhu.edu.cn

mgg1@ualberta.ca

Text S1. Characterization

The morphological features and particles size of the prepared catalyst nanoparticles were observed by field emission scanning electron microscope (FESEM, Zeiss Gemini SEM560), and the elemental distribution of the catalyst surface was obtained by an energy-dispersive X-ray spectrometer (EDS). The chemical composition and the phase structure of the catalysts and membranes were measured by using the X-ray photoelectron spectroscopy (XPS, Escalab 250Xi, Thermo Fisher), Fourier transform infrared (FTIR, NicoletIn10M, Thermo Fisher) spectra and X-ray diffractometer (XRD, D8-Advaced, Bruker, Germany). The Automated Area and Pore Size Analyzer (Autosorb-iQ) was employed to measure the N₂ adsorption-desorption isotherms of the catalyst samples. The Brunauer-Emmett-Teller (BET) surface area and porous structures of samples were calculated by the Brunauer-Emmett-Teller (BET) and Barrett-Joyner-Halenda (DFT) methods, respectively. The Shimadzu analyzer (TOC-L Shimadzu) was used to investigate the concentration of total organic carbon (TOC) of the water samples. The $\cdot\text{OH}$, $\text{SO}_4^{\cdot-}$, $\text{O}_2^{\cdot-}$ and $^1\text{O}_2$ was detected by electron paramagnetic resonance spectrometer (ERP, Bruker EMXplus) and the DMPO (50 μM) and TEMP (100 μM) was employed as spin trapping agent of $\cdot\text{OH}/\text{SO}_4^{\cdot-}$, $\text{O}_2^{\cdot-}$ and $^1\text{O}_2$, respectively. The detailed test process is similar to the previous reports ¹.

Text S2 Adsorption performance

100 mg/L adsorbents (CU4F) were added to sulfamethoxazole and caffeine solution with the initial concentration of 10-80 mg/L ($V = 100$ mL) in 150 mL flask for the batch experiments. The above samples were placed in the constant temperature oscillator at 150 r/min with the temperature of 25 °C, sampling at 240 min, and all the collected solution were filtered with a 0.45 μ m membrane filter and the concentrations of sulfamethoxazole and caffeine were determined by UV spectrophotometer at 265 and 275 nm, respectively. All of the experiments were performed in triplicates. The concentrations of samples at equilibrium were measured and the adsorption capacity of adsorbents was calculated by Eq. S1 as follow:

$$q_t = \frac{(C_0 - C_t)V}{m} \quad (1)$$

where C_0 (mg/L) and C_t (mg/L) were the concentrations of sulfamethoxazole at initial and t time (min), q_t (mg/g) was the adsorption amount at t time (min).

Langmuir isotherms model:

$$\frac{C_e}{q_e} = \frac{C_e}{q_0} + \frac{1}{K_L q_0} \quad (2)$$

where C_e represents the equilibrium concentration on sulfamethoxazole and caffeine (ppm), q_e represents the equilibrium adsorption capacity on sulfamethoxazole and caffeine (mg/g), q_0 represents the theoretical maximum adsorption capacity on sulfamethoxazole and caffeine (mg/g), and K_L (L/mg) represents the Langmuir constant related to the enthalpy of adsorption, respectively

Freundlich isotherms model:

$$\ln q_e = \ln k_F + \frac{\ln c_e}{n} \quad (3)$$

where K_F (mg/g) represents the Freundlich constant that shows adsorption uptake related to bond strength, and n represents Freundlich exponent which shows the adsorption intensity or surface heterogeneity.

Temkin isotherms model:

$$q_e = \frac{RT}{b_T} \ln k_e + \frac{RT}{b_T} \ln C_e \quad (4)$$

R (8.314 J mol⁻¹ K⁻¹) was the gas constant, b_T expresses the bond energy representing the type of bond sulfamethoxazole.

Pseudo-first-order models:

$$\ln (q_e - q_t) = \ln q_e - k_1 t \quad (5)$$

Pseudo-second-order models:

$$\frac{t}{q_t} = \frac{1}{k_2 q_e^2} + \frac{t}{q_e} \quad (6)$$

where q_e and q_t (mg/g) represent the adsorption capacity at equilibrium and at a specified time (min), respectively. k_1 (min⁻¹) and k_2 (g/(mg min)) represent the rate constant of pseudo-first-model and pseudo-second-model, respectively.

Intraparticle diffusion model

The intraparticle diffusion mechanism can be analyzed using the diffusion model described by the following equation:

$$q_t = K_i t^{\frac{1}{2}} + C \quad (7)$$

where k_i (mg/(g min^{1/2})) was the intraparticle diffusion rate constant and C (mg/g) was a measure of the thickness of the boundary layer.

Text S3. Catalytic performance

The catalytic performance of the prepared products was tested in 100 mL mixed solution containing pollutants and PMS at 25 °C. In a typical experiment, a certain amount of catalyst and PMS were sequentially added into pollutants solution. Afterwards, 1 mL of aqueous sample was obtained from above solution by using 0.22 μm nylon syringe filters at required time intervals (3 min), which quickly mixed with 1 mL methanol to quench the catalytic reaction. The concentration of pollutants was detected by HPLC (Agilent 1260, America) with a Gemini 5u C18 110A reverse phase (150 mm \times 4.6 mm). The mobile phase consisted of a dual eluent system, comprising (A) water with 0.1% acetic acid and (B) acetonitrile containing 0.1% acetic acid, flowing at a rate of 0.4 mL/min. The concentration of mobile phase and peaks of pollutants were listed in Table S1.

Table S1. The HPLC analytical method of different organic contaminants

Sample	Mobiles phase %		Wavelength (nm)	Flow (mL/min)
	water	acetonitrile		
Sulfamethoxazole	90	10	265	0.4
Ibuprofen	60	40	220	
Caffeine	95	5	275	
Bisphenol A	70	30	280	
Atrazine	70	30	225	
Carbamazepine	75	25	210	

The influence factors of catalyst dosage, initial pH value, PMS concentration, anions (20 mM of SO_4^{2-} , H_2PO_4^- and HCO_3^-) and organic matter (10 ppm humic acid) on the degradation efficiency of sulfamethoxazole and caffeine were systematically investigated. The pH value of sulfamethoxazole solution (3-11) was adjusted by 0.1 M H_2SO_4 or 0.1 M NaOH solution. For the reusability and stability of the prepared catalysts, the catalysts were collected by centrifugation after catalytic reaction, and washed with deionized water for 3 times and methanol 3 times respectively, and then

dried at 60 °C. Subsequently, the samples were employed to be reused for the same procedure mentioned above. In addition, the tert-Butanol (TBA, 100 mM), methanol (100 mM), p-benzoquinone (10 mM) and furfuryl alcohol (FFA, 2 mM) were employed to investigate the prominent reactive oxygen species.

The dynamic catalytic activity of CU4F-based nanofibrous membranes was investigated by the designed dead-end filtration device under gravity. As shown in Figure 9a, a circular membrane was put in a vertical cell and the pollutants solution (10 µM) containing 1mM PMS was poured into the cell by peristaltic pump. The volume of the permeation solution and concentration of sulfamethoxazole were immediately measured at several times.

The quantitative analysis of all pollutants in the mixture was carried out by an Agilent 1290 Infinity II UHPLC system coupled to an Agilent 6495 triple quadrupole mass spectrometer (QQMS, Agilent Technologies Inc, Canada). Agilent Poroshell 120 EC-C18 (2.1 × 50 mm, 1.9 µm) column was used for chromatographic separation with mobile phases of water with 0.1% acetic acid (A) and acetonitrile with 0.1% acetic acid (B). The elution gradient was 0-0.5 min, 0% B; 0.5-5 min, increased from 0% B to 100% B; 5.5 min, decreased to 0% B and held at 0% B for 5 min to equilibrate column with a flow rate of 0.4 mL/min. The column temperature was set at 40 °C throughout the run. The samples were analyzed with an injection volume of 10 µL.

Text S4. Analytical methods.

The pseudo first-order kinetic model Eq. S8 was used to fit pollutants degradation in PMS system experiments.

$$\ln (C_t/C_0) = -k \cdot t \quad (8)$$

C_t represented pollutant concentrations at precis designed sample time t , and C_0 represented for initial pollutant concentration. k was the rate constant of pseudo first-order reaction.

PMS concentration

Typically, 0.2 mL sample was added to a mixed solution containing 1 mL of 40 mM FeSO₄, 0.4 mL of 100 mM NDPDAS and 8.4 mL of deionized water at pH 3, shaken immediately for color to develop, and measured at $\lambda_{\text{adsorption}}=510$ nm on UV-vis spectrophotometer.

Text S5. Intermediates analysis

The intermediates of sulfamethoxazole degradation were determined by high-performance LC-MS/MS (Agilent 1290UPLC) equipped with electrospray ionization (ESI). A waters BEH C18-WP (2.1 mm × 100 mm × 1.7 μm) was used as the chromatography column, and the temperature of the column was maintained at 30 °C. The mobile phase was a mixture of two solutions, namely A and B. Eluent A is made of 0.5 vol% formic acid in methanol and eluent B is methanol. Test conditions: capillary voltage 4 kV; gas temperature 350 °C. MS was performed in the positive ion mode with an electrospray ionization (ESI) source. MS was scanned at a mass range from 50 to 1000 m/z (scanning current: 20 A).

Text S6. Electrochemical tests

All the electrochemical measurements were conducted at room temperature in a three-electrode system controlled by a CHI660E electrochemical station. Firstly, 5 mg of CU4F catalysts was added into 1 ml N,N-dimethylformamide solution containing 5 wt% Nafion perfluorinated resin, followed by stirring and ultrasonication for 30 min, the mixed solution was dropped on a glassy carbon electrode (GCE) and placed into an oven at 40 °C for 30 min. Catalysts coated glassy carbon electrode were utilized as the working electrodes. Ag/AgCl electrode and Pt wire electrode were used as reference electrode and counter electrode, respectively. Electrochemical impedance spectroscopy (EIS) tests were carried out at open circuit potential in 0.5 M Na₂SO₄ with a frequency range from 10⁶ to 0.005 Hz. In open circuit potential test, PMS (1 mM) and pollutants (0.05 mM) were injected into the system, respectively, at a certain time. Temporal change in the open-circuit potential (OCP) was monitored under the maximal current not exceeding 500 nA.

Test S7. DFT calculations

Potential reactive sites were predicted based on DFT. First, we calculated the distributions of the lowest unoccupied molecular orbital (LUMO), highest occupied molecular orbital (HOMO), and surface ionization energy (ALIE) of sulfamethoxazole to provide an initial evaluation of the vulnerable areas for nucleophilic and electrophilic reactions. Furthermore, condensed Fukui functions, including the nucleophilic index (f^+), electrophilic index (f^-), radical attack index (f^0), and condensed dual descriptors (CDD), were calculated to predict the reactive sites.

DFT calculations were performed using the Gaussian 09 package, following the works of Liu et al. ². The geometrical parameters of sulfamethoxazole were established without symmetry constraints. All calculations were performed using Becke's three-parameter hybrid functional with the LYP correlational functional (B3LYP) at the 6-31 G (d, p) basis set level, taking into account dispersion correction (D3(BJ)). Four default convergence parameters (root-mean-square force, root-mean-square displacement, maximum force, and maximum displacement) in the Gaussian program were used to perform geometric optimization and frequency analysis. The results of the frequency analysis confirmed that all geometries were real minima with no imaginary frequencies. The wave function of the sulfamethoxazole molecule was calculated using Multiwfn 3.7, and data were visualized using Visual Molecular Dynamics.

Test 8. Contribution of ROSs

Inhibition of scavengers

The inhibition effect of pollutants degradation by four scavengers were calculated with the following equation ³:

$$[\bullet\text{OH}] = (k_0 - k_2)/k_0 \times 100\% \quad (9)$$

$$[\text{SO}_4^{\bullet-}] = (k_2 - k_1)/k_0 \times 100\% \quad (10)$$

$$[\text{O}_2^{\bullet-}] = (k_0 - k_3)/k_0 \times 100\% \quad (11)$$

$$[{}^1\text{O}_2] = (k_0 - k_4)/k_0 \times 100\% \quad (12)$$

Where k_0 was the reaction rate without any quenching agents, k_1 , k_2 , k_3 and k_4 were pollutants degradation rates in the presence of MeOH, TBA p-BQ and FFA, respectively.

Quantitation of ROSs

The furfuryl alcohol (FFA), nitrobenzene (NB) and benzene acid (BA) were used as probe to carry out the quantitative experiments of ROS.

The apparent rate constant (k_{app}) was calculated according to Eq. S8:

$$\ln(C_t/C_0) = -k_{app} \cdot t \quad (13)$$

where C_0 and C_t were concentrations of pollutant (mg L^{-1}) at time zero and time t min, t was the electrolysis time in min, and k_{app} was the apparent rate constant (min^{-1}).

The steady-state concentrations of $\bullet\text{OH}$ ($[\bullet\text{OH}]_{ss}$), $\text{SO}_4^{\bullet-}$ ($[\text{SO}_4^{\bullet-}]_{ss}$) and ${}^1\text{O}_2$ ($[{}^1\text{O}_2]_{ss}$) in the CU4F/PMS system was measure by furfuryl alcohol (FFA), nitrobenzene (NB) and benzene acid (BA) as a probe molecule for $\bullet\text{OH}$, $\text{SO}_4^{\bullet-}$ and ${}^1\text{O}_2$, respectively ⁴. The second-order rate constant of reaction of NB with $\bullet\text{OH}$ is higher ($k_{NB,\bullet\text{OH}}=3.9 \times 10^9 \text{ M}^{-1}\text{s}^{-1}$) compared with $\text{SO}_4^{\bullet-}$ ($k_{NB,\text{SO}_4^{\bullet-}} \leq 10^6 \text{ M}^{-1}\text{s}^{-1}$), whereas the second-order rate constant of the reaction of BA with both $\bullet\text{OH}$ ($k_{BA,\bullet\text{OH}}=2.1 \times 10^9 \text{ M}^{-1}\text{s}^{-1}$) and $\text{SO}_4^{\bullet-}$ ($k_{BA,\text{SO}_4^{\bullet-}}=1.2 \times 10^9 \text{ M}^{-1}\text{s}^{-1}$) was quite similar and higher. FFA has a higher rate constant with ${}^1\text{O}_2$ ($k_{FFA,{}^1\text{O}_2}=1.2 \times 10^8 \text{ M}^{-1}\text{s}^{-1}$), $\bullet\text{OH}$ ($k_{FFA,\bullet\text{OH}}=1.5 \times 10^{10} \text{ M}^{-1}\text{s}^{-1}$) and $\text{SO}_4^{\bullet-}$ ($k_{FFA,\text{SO}_4^{\bullet-}}=1.5 \times 10^{10} \text{ M}^{-1}\text{s}^{-1}$).

$k_{FFA,SO_4^{\bullet-}} \sim 10^6 \text{ M}^{-1}\text{s}^{-1}$). The $[\cdot\text{OH}]_{ss}$, $[\text{SO}_4^{\bullet-}]_{ss}$ and $[^1\text{O}_2]_{ss}$ were obtained as follows :

$$[\cdot\text{OH}]_{ss} = \frac{k_{app, NB}}{k_{NB, \cdot\text{OH}}} \quad (14)$$

$$[\text{SO}_4^{\bullet-}]_{ss} = \frac{k_{app, BA} - [\cdot\text{OH}]_{ss} \times k_{BA, \cdot\text{OH}}}{k_{BA, SO_4^{\bullet-}}} \quad (15)$$

$$[^1\text{O}_2]_{ss} = \frac{k_{app, FFA} - [\cdot\text{OH}]_{ss} \times k_{FFA, \cdot\text{OH}} - [\text{SO}_4^{\bullet-}]_{ss} \times k_{FFA, SO_4^{\bullet-}}}{k_{FFA, ^1\text{O}_2}} \quad (16)$$

Where $k_{app, NB}$, $k_{app, BA}$, and $k_{app, FFA}$ are the apparent rate constants for the degradation of NB, BA, and FFA, respectively.

Test 9 Microtox® assay

Luminescence intensity was measured at 15 °C after 0, 45 and 90 min using a Microtox® 500 analyzer (Strategic Diagnostics Inc., Delaware, USA). Before starting the bioassays, the cuvettes with saline diluent were pre-equilibrated in the analyzer to the 15 °C test temperature. The pH value of samples should be 6.8-7.2 by using 1.0 M NaOH or HCl solutions. Negative and positive controls were diluent (NaCl, 2 %) and 100 mg/L of phenol.

First, the *Aliivibrio fischeri* reagent was reconstituted by adding cooled (4 °C) 1 mL reconstitution solution (RS) into the lyophilized bacteria. 20 µL diluted bacteria reagents were added to a luminescent plate on the cooling block. After 15 min, the luminescence was detected and named as I₀. 180 µL samples and phenol were then transferred to the luminescent plate. The luminescence was measured at 30 min and 60 min, which were named as I₃₀ and I₆₀.

The inhibition effect (%) was calculated as below:

$$R_t = \frac{I_{ct}}{I_{ci}} \quad (17)$$

$$G_t = \frac{R_t \times I_{si}}{I_{si}} - 1 \quad (18)$$

$$\text{inhibition effect (\%)} = \frac{G_t}{1 + G_t} \times 100\% \quad (19)$$

- First is to get the correction factor (R_t) using the signals from negative control (Diluent as the control);
- Second is to get Gamma (G_t) using R_t and the signal from the sample;
- Third is to convert G_t to inhibition effect (%);

Where R_t corrects for any inhibition induced by the negative control sample and I_{ct} and I_{ci} are the absolute light intensities produced by the negative control at time t and at the initial time, i , respectively. In addition, I_{si} and I_{st} are the light intensities produced by the water sample at the initial time, i , and time t , respectively.

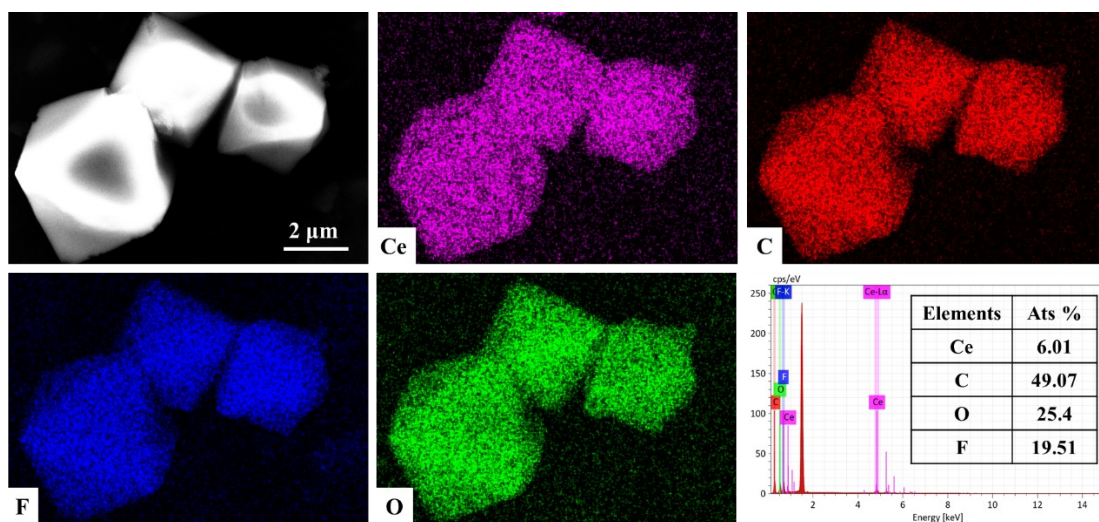


Figure S1. The elements mapping (Ce, C, F and O) and content of CU₄F catalysts.

Table S2. The BET surface area, average pore diameter and BJH pore volume of the CU4F catalysts.

Sample	BET surface area (m ² /g)	Pore volume (cm ³ /g)	Pore diameter (nm)
CU4F	669.85	0.393	3.054

Table S3. The defect density of Ce to BDC-X (X = F and H) in the CUH and CUF

Sample	Weight (mg)	Ce (μmol)	BDC-X (μmol)	Ce: BDC-X	Defect density (%)
CUF	10	20.8	10.06	6:3.45	42.5

samples

The ligand defect density values of four Ce-UiO-66-X samples were obtained via the integration of the Ce contents extracted from ICP-OES and the ligand contents given in quantitative ^1H NMR spectra (Figure 2b). The molar ratio in the ideal Ce-UiO-66-X crystal ($\text{Ce}_6(\text{OH})_4\text{O}_4(\text{BDC-X})_6$) was 6:6.

The defect density was calculated with the following equation:

$$\text{The defect density (\%)} = \frac{6 - \text{mole}_{(\text{BDC-X})}}{6} \times 100\% \quad (20)$$

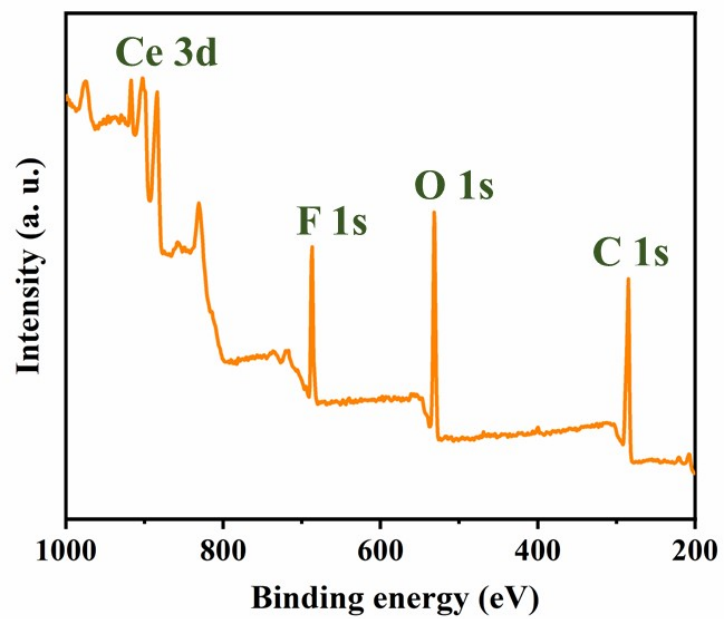


Figure S2. The XPS spectra of CU4F catalysts.

Table S4. Fractions of different element species in CU4F.

	Ce (%)			O (%)		
	Ce ³⁺	Ce ⁴⁺	Ce ³⁺ /Ce ⁴⁺	O _L	O _C	O _{OH}
CUF	29.7	70.3	0.42	13.5	63.5	23

Table S5. Isotherms parameters for sulfamethoxazole and caffeine adsorption onto CU4F.

Adsorbents	Langmuir			Freundlich			Temkin		
	q_m (mg/g)	K_L (L/mg)	R^2	K_F (mg/g)	$1/n$	R^2	b_T	K_L (L/mg)	R^2
sulfamethoxazole	305.8	0.045	0.981	26.6	0.538	0.986	36.4	0.447	0.965
caffeine	54.1	0.007	0.826	0.59	0.819	0.985	309.5	0.14	0.937

Table S6. Adsorption kinetics parameters for sulfamethoxazole and caffeine adsorption onto CU4F.

Samples	Pseudo-first-order kinetic model			Pseudo-second-order kinetic model		
	q_e (mg/g)	k_1 (min ⁻¹)	R^2	q_e (mg/g)	k_2 (g·mg ⁻¹ ·min ⁻¹)	R^2
sulfamethoxazole	120.05	0.0403	0.918	212.31	9.38×10^{-4}	0.999
caffeine	21.87	0.0205	0.975	28.61	1.39×10^{-3}	0.999

Table S7. The parameters of intraparticle diffusion model for CU4F.

Absorbents	External diffusion			Intraparticle diffusion			Adsorption equilibrium		
	k_1 (mg/(g·min ^{1/2}))	C (mg/g)	R^2	k_{II} (mg/(g·min ^{1/2}))	C (mg/g)	R^2	k_{III} (mg/(g·min ^{1/2}))	C (mg/g)	R^2
sulfamethoxazole	18.23	88.74	0.968	5.52	142.5	0.984	0.41	201.5	0.982
caffeine	4.34	4.44	0.987	1.69	5.88	0.984	0.44	19.12	0.984

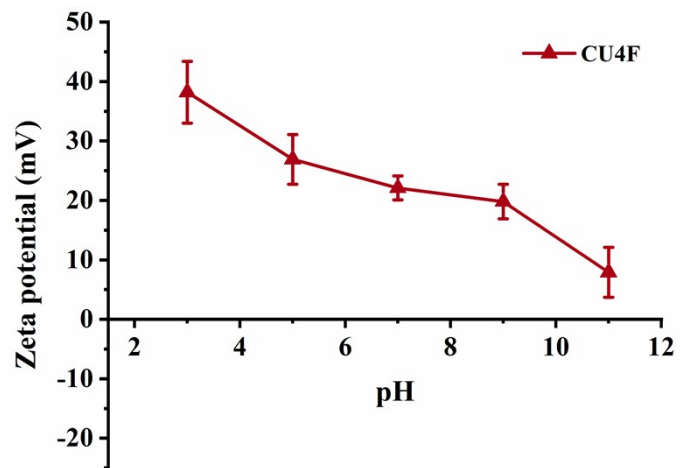


Figure S3. Zeta potential of CU4F catalysts.

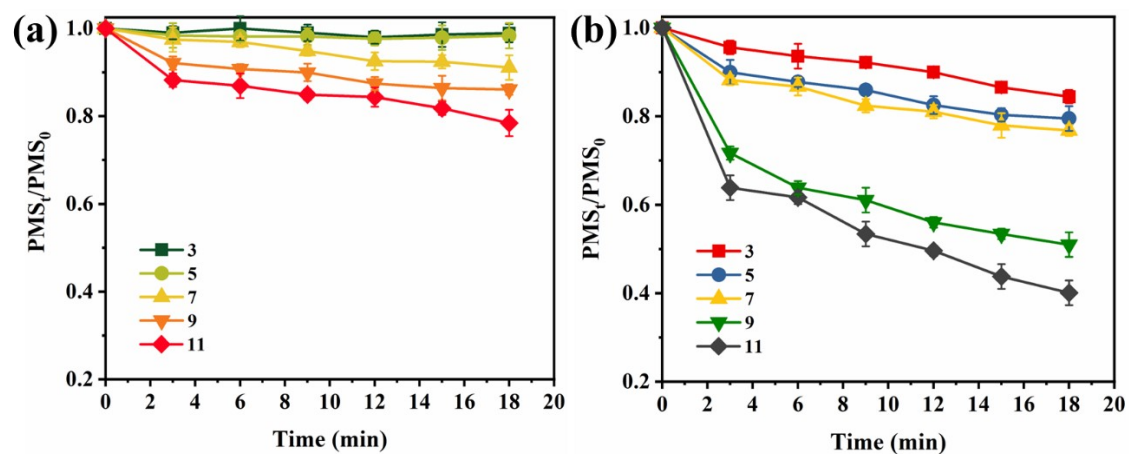


Figure S4. Effect of pH on PMS consumption without and with CU4F catalyst.

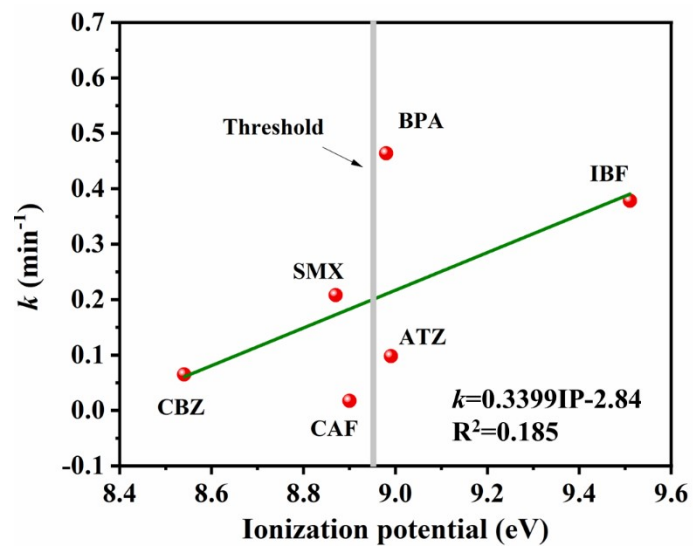


Figure S5. Correlation of k to ionization potential of CU4F catalysts.

Table S8. Water quality parameters of the second effluent water and Tap water (water samples were filtered by the 0.45 μm membranes to remove the particulate matters).

	Water sample	
	Tap water	Second effluent water
pH	7.6	8.3
COD (mg/L)	10.22	36.3
TOC (mg/L)	18.4	40.2
Conductivity ($\mu\text{S}/\text{cm}$)	428	933
Cl^- (mg/L)	15.88	45.4
SO_4^{2-} (mg/L)	6.35	125.2
NO_3^- (mg/L)	120.2	728.2
H_2PO_4^- (mg/L)	1.10	3.45

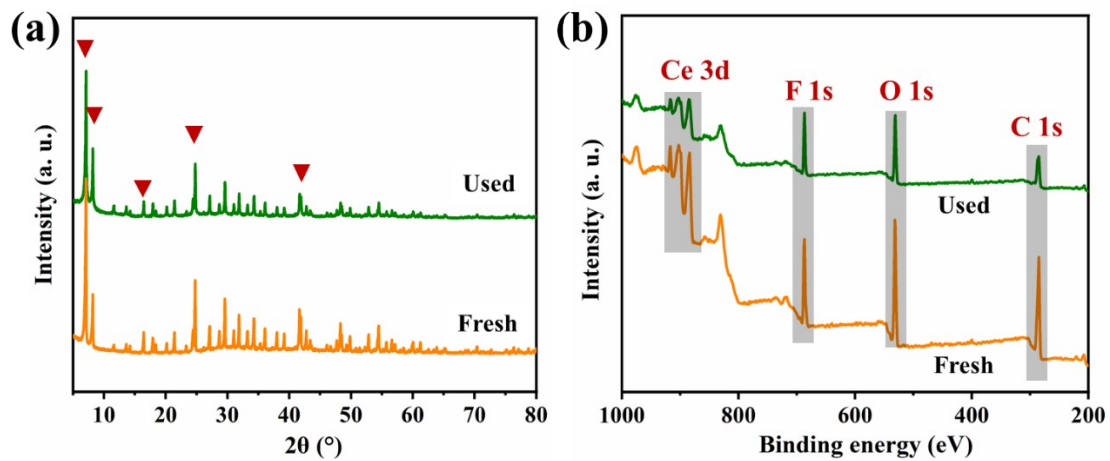


Figure S6. XRD pattern (a) and XPS spectra (b) of the fresh and used CU4F catalysts.

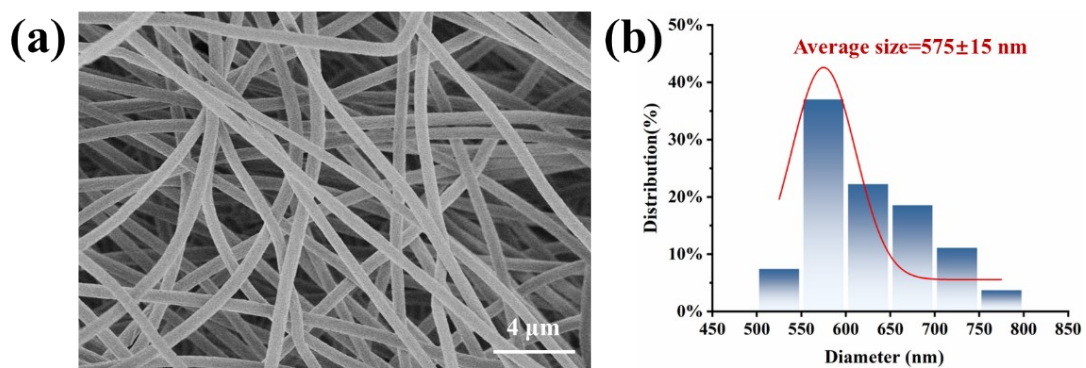


Figure S7. The surface SEM images (a) and fiber diameter distribution (b) of PAN NFMs.

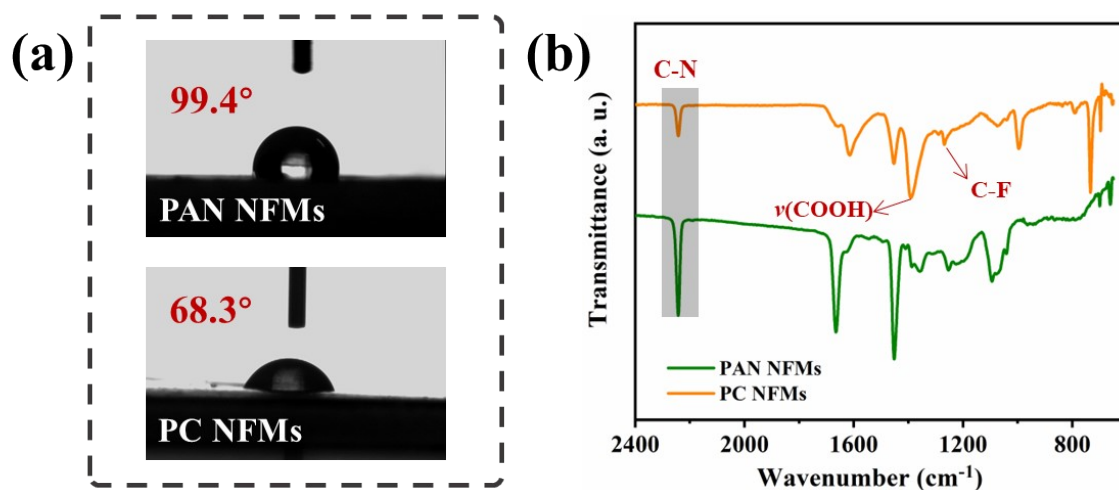


Figure S8. The water contact angles (a) and FT-IR spectra (b) of PAN NFMs and PC NFMs.

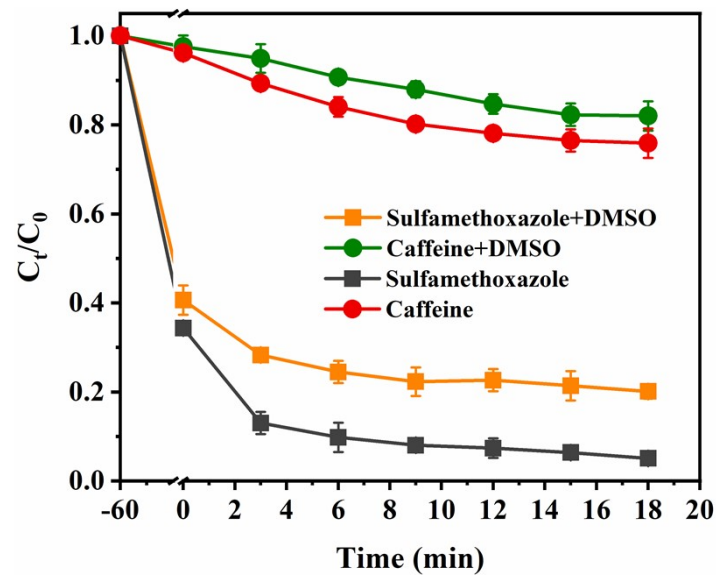


Figure S9. Effect of DMSO on the removal efficiency of CU4F/PMS. Condition: CU4F=100 mg/L, PMS=1 mM and DMSO=10 μ M.

	Sulfamethoxazole	Caffeine
TBA	35.4%	84.9%
MeOH	48.3%	86.4%
p-BQ	20.6%	72.9%
FFA	78.1%	89.3%
DMSO	61.8%	37.7%

Table S9. The inhibition effect of scavengers on the CU4F/PMS system

Table S10 The steady-state concentrations and second-order kinetics of reactive species in

	NB	BA	FFA
k_{app} (s ⁻¹)	1.20	2.04	5.39
	[·OH] _{ss}	[SO ₄ ^{·-}] _{ss}	[¹ O ₂] _{ss}
C (×10 ⁻¹⁰ M)	3.1	11.6	65.2
	k_{abs} ·OH (M ⁻¹ s ⁻¹)	k_{abs} SO ₄ ^{·-} (M ⁻¹ s ⁻¹)	k_{abs} ¹ O ₂ (M ⁻¹ s ⁻¹)
sulfamethoxazole	6.0×10 ⁹	16.1×10 ⁹	2×10 ⁴
caffeine	6.4×10 ⁹	2.4×10 ⁹	3×10 ⁸

the CU4F/PMS system

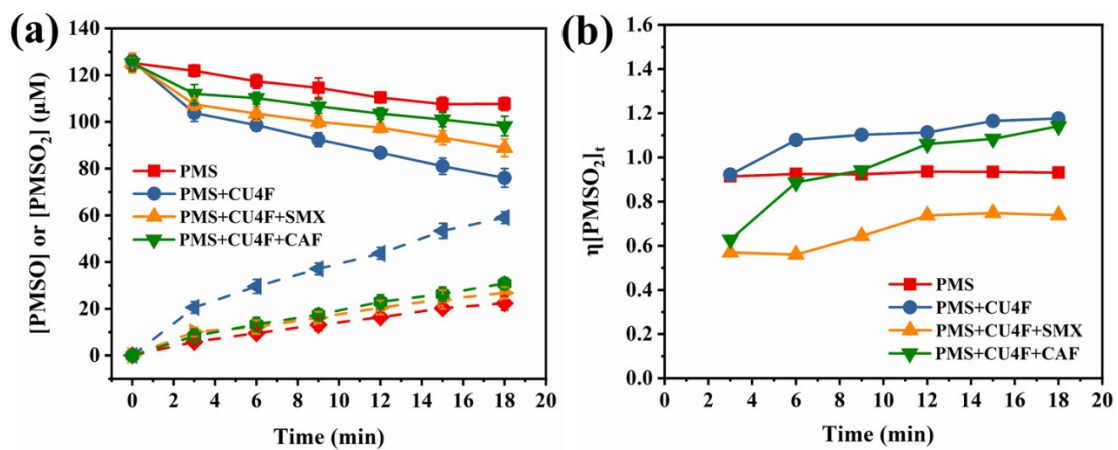


Figure S10. (a) The PMSO consumption and PMSO₂ generation in CU4F/PMS system. (b) The yield of PMSO₂ in CU4F/PMS system. Condition: CU4F=100 mg/L, PMS=1 mM and PMSO=125 μM.

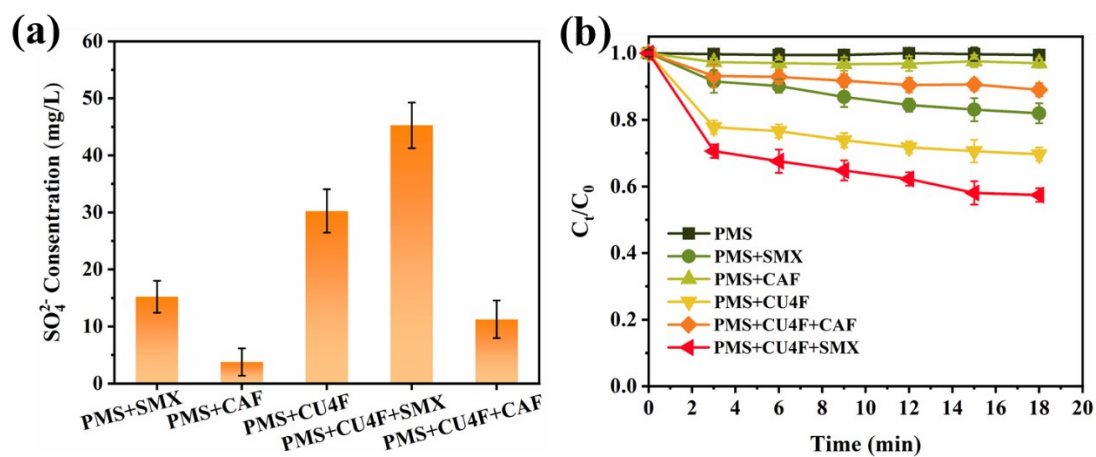


Figure S11. The SO₄²⁻ generation (a) and PMS consumption (b) in different reaction system. Condition: PMS=1 mM, CU4F=100 mg/L and pollutants= 50 μM.

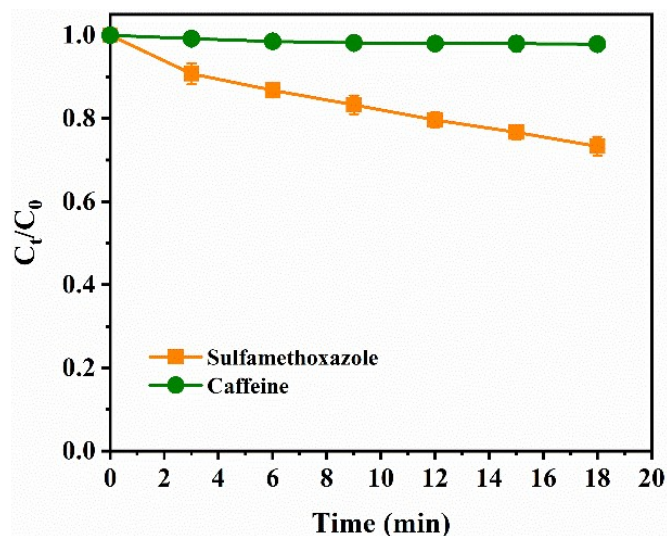


Figure S12. The removal efficiency of PMS without catalysts. Condition: PMS=1 mM and pollutants= 50 μ M.

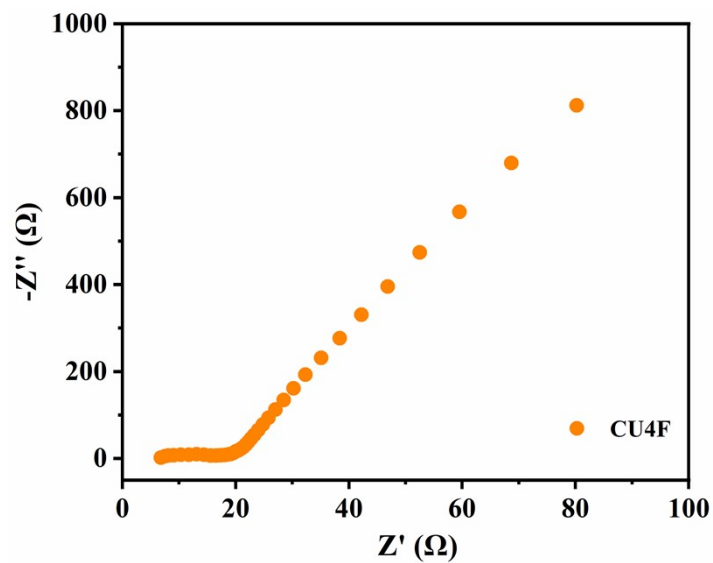


Figure S13. Electrochemical impedance spectroscopy (EIS) Nyquist plot of CU4F catalyst.

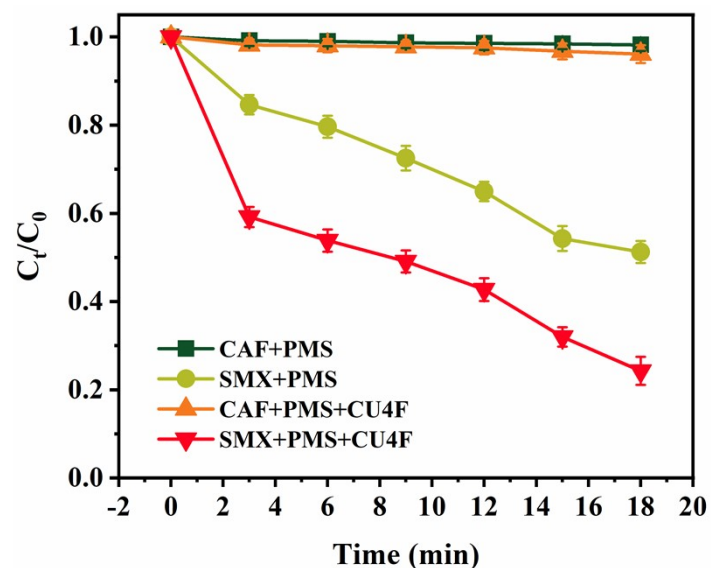


Figure S14. The sulfamethoxazole and caffeine degradation efficiency of GOS

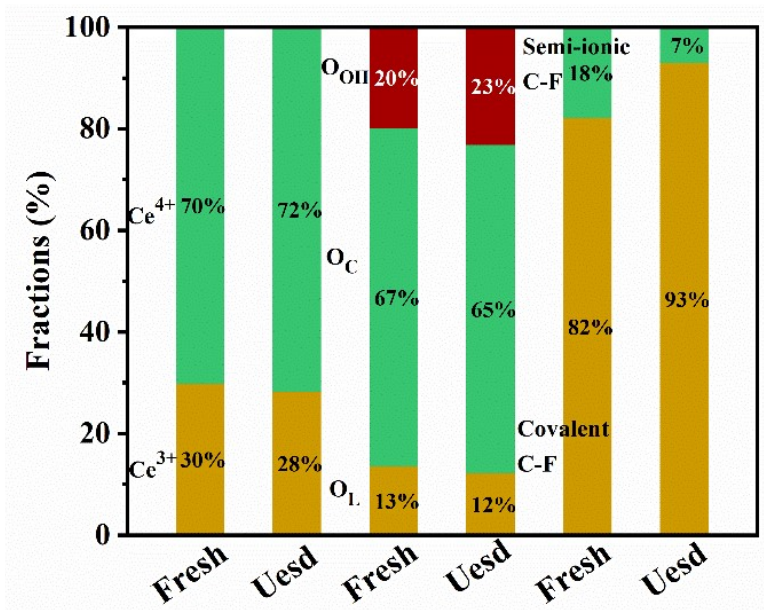


Figure S15. XPS Ce 3d, O 1s and F 1s of the fresh and used CU4F.

Table S11. The Fukui index of sulfamethoxazole (the deeper color presented the higher Fukui index, reflecting the attractive attacked sites.).

Atom	f^+	f^-	f^0	CDD
C1	0.0069	0.01	0.0084	0.0031
C2	0.0153	0.0262	0.0207	0.0109
C3	0.0016	0.0062	0.0039	0.0046
C4	-0.002	0.0053	0.0017	0.0073
N5	0.026	0.0251	0.0255	-0.0009
O6	0.0245	0.0262	0.0254	0.0017
N7	0.0463	0.0159	0.0311	-0.0304
S8	0.015	0.0182	0.0166	0.0032
O9	0.0398	0.0312	0.0355	-0.0086
O10	0.0387	0.0305	0.0346	-0.0082
C11	0.0878	0.0262	0.057	-0.0616
C12	0.0354	0.0708	0.0531	0.0354
C13	0.0717	0.1025	0.0871	0.0308
C14	0.0571	0.0393	0.0482	-0.0178
C15	0.0679	0.0883	0.0781	0.0204
C16	0.0379	0.1047	0.0713	0.0668
N17	0.1432	0.029	0.0861	-0.1142
H18	0.008	0.0103	0.0092	0.0023
H19	0.0072	0.0125	0.0099	0.0053
H20	0.0138	0.0175	0.0156	0.0037
H21	0.0069	0.0089	0.0079	0.002
H22	0.016	0.0222	0.0191	0.0062
H23	0.0274	0.0379	0.0326	0.0105
H24	0.036	0.0612	0.0486	0.0252
H25	0.0357	0.0522	0.044	0.0165
H26	0.0295	0.0577	0.0436	0.0282
H27	0.0529	0.033	0.043	-0.0199
H28	0.0533	0.0293	0.0413	-0.024

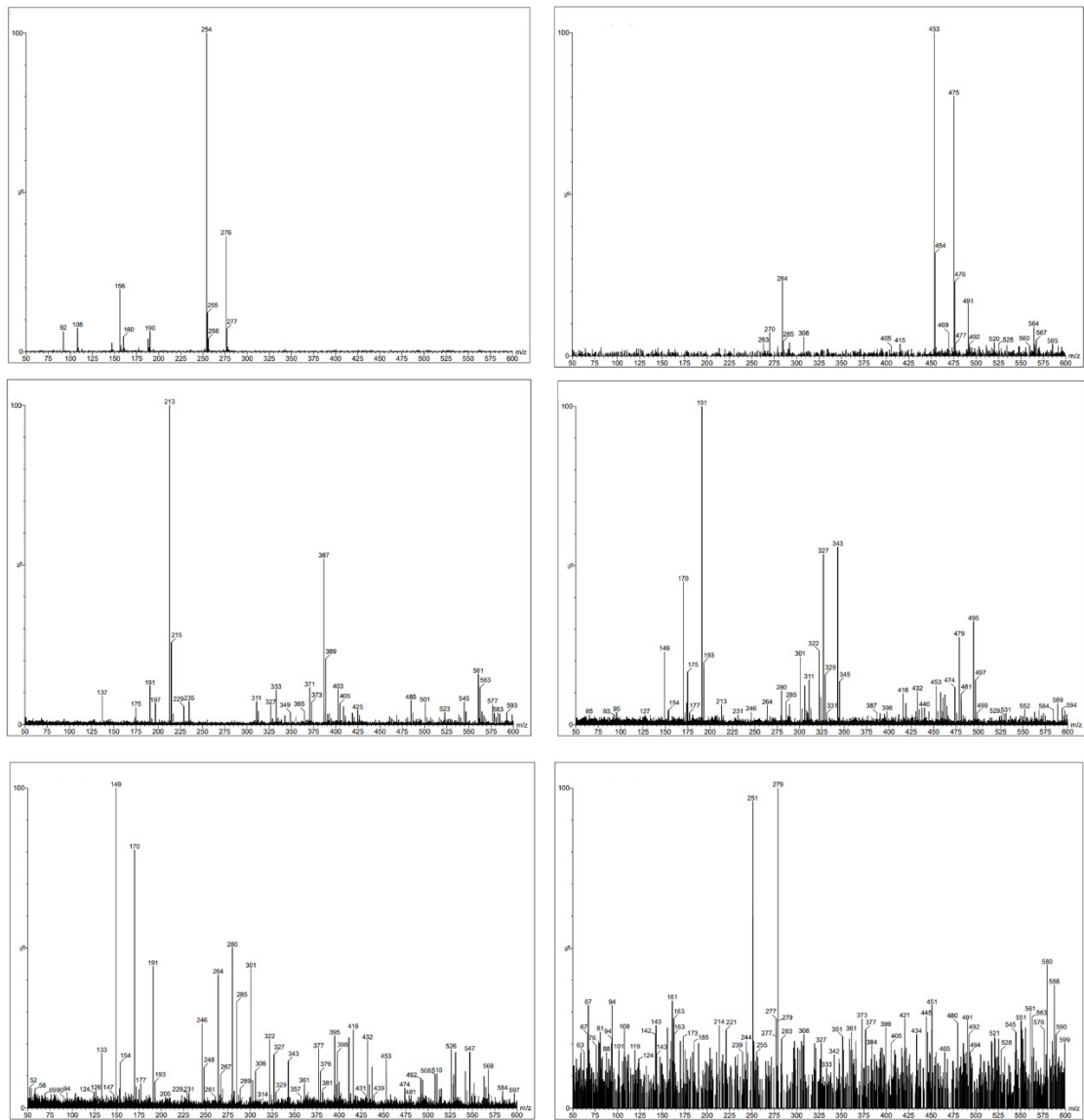


Figure S16. The mass spectra of sulfamethoxazole and its intermediates.

	45 min	90 min
Sulfamethoxazole	70.5%	83.2%
CU4F/PMS	62.9%	69.5%

Table S12. The inhibition effect of sulfamethoxazole and CU4F/PMS.

Reaction formulas involved in the text

(1) The effect of pH on PMS activity



(2) The effect of Cl^- , HCO_3^- , and H_2PO_4^- on PMS activity



(3) Ce activate PMS to produce ROSs.



References

1. Z. Huang, Q. Zeng, Y. Liu, Y. Xu, R. Li, H. Hong, L. Shen and H. Lin, *Journal of Membrane Science*, 2021, **640**, 119854.
2. D. Wang, T. Zhang, M. Gamal El-Din and X. Wang, *Chemical Engineering Journal*, 2024, **500**, 156624.
3. X. Li, Y. Hu, C. Zhang, C. Xiao, J. Cheng and Y. Chen, *Journal of Hazardous Materials*, 2023, **442**, 130016.
4. S. O. Ganiyu, N. A. S. Hussain, J. L. Stafford and M. Gamal El-Din, *Chemical Engineering Journal*, 2024, **480**, 147737.